Waveguide loss reduction of GaInAsP/InP membrane lasers by reduction of doping concentration of *p*-InP cladding layer

T. Tomiyasu[1], T. Hiratani[1], D. Inoue[1], N. Nakamura[1], T. Amemiya[1, 2], N. Nishiyama[1, 2], and S. Arai[*1, 2]

[1]*Department of Electrical and Electronic Engineering, Tokyo Institute of Technology, O-okayama, Meguro, Tokyo 152-8552, Japan*

[2]*Institute of Innovative Research (IIR), Tokyo Institute of technology, O-okayama, Meguro, Tokyo 152-8552, Japan*

In order to realize on-chip optical interconnections, we proposed and demonstrated membrane DFB and DR lasers for low-power-consumption operation [1-2]. However, light output was not enough for desired system due to high waveguide loss α_{WG} of 42 cm^{-1} [3]. In this work, we investigated on the waveguide loss reduction of membraned lasers.

Figure 1 shows the cross sections of a membrane laser with core thickness of 270 nm including low doped *p*-InP cap layer ($N_{A,cap}$ = 3×10^{17} cm^{-3}) for the decrease of absorption coefficients of *p*-InP. In this work, we fabricated membrane FP lasers with lower ($N_{A,\,p\text{-clad.}}$ = 5×10^{17} cm^{-3}: Device I) doping concentration of *p*-InP side cladding layer and compared with previously reported devices with relatively high doping concentration ($N_{A,\,p\text{-clad.}}$ = 2×10^{18} cm^{-3}: Device II). Since the mode field of the membrane laser tends to spread in horizontal direction due to high-index-contrast structure as shown in Fig. 2, the reduction of *p*-InP doping concentration is considered to effective for reduction of the waveguide loss. The absorption losses in the *p*-InP layers of Devices I and II were calculated to be 1.1 cm^{-1} and 4.5 cm^{-1}, respectively, while that of conventional (vertical injection type) BH lasers was 2.4 cm^{-1}.

Figure 3 shows the current–light output and current–voltage characteristics of the fabricated devices. The stripe width and the cavity length of Device I were 0.6 μm and 830 μm, respectively, and these of Device II were 0.7 μm and 900 μm, respectively. The threshold current I_{th} of 4.0 mA, external differential quantum efficiency η_d of 16% and differential resistance dV/dI of 38 Ω were obtained in Device I, while I_{th} of 5.6 mA, η_d of 13% and dV/dI of 28 Ω were obtained in Device II. As can be seen in Fig. 4, we obtained an internal quantum efficiency, η_i, of 75% for the both devices and the waveguide loss, α_{WG}, of 22 cm^{-1} for Device I, and α_{WG} of 31 cm^{-1} for Device II. Figure 5 shows the waveguide loss dependence on the doping concentration of *p*-InP cap layer. The waveguide loss reduction due to lower concentration of *p*-InP layers was confirmed. Figure 6 shows the cavity length dependence of the differential resistance. Although the differential resistance was increased by about 1.5 times, it can be reduced in proportion to the distance from *p* side electrode to the active region.

References

[1] T. Okamoto *et al.*, "Optically pumped membrane BH-DFB lasers for low-threshold and single-mode operation," *IEEE J. Sel. Topics Quantum Electron.*, vol. 9, no. 5, pp. 1361–1366, Sept./Oct. 2003.

[2] T. Hiratani *et al.*, "Room-temperature continuous-wave operation of membrane distributed-reflector laser," *Appl. Phys. Express*, vol. 8, no. 11, pp. 112701, Sept./Oct. 2015.

[3] D. Inoue *et al.*, "Room-temperature continuous-wave operation of GaInAsP/InP lateral-current-injection membrane laser bonded on Si substrate," *Appl. Phys. Express*, vol. 7, no. 7, pp. 072701, May/June 2014.

*Corresp. author: arai@pe.titech.ac.jp, Phone: +81-03-5734-2512, Fax: +81-03-5734-2907

Figures

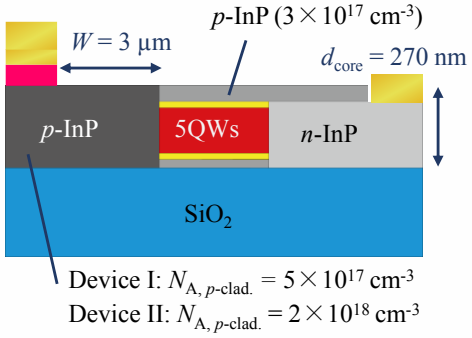

Fig. 1. Cross section of a membrane laser.

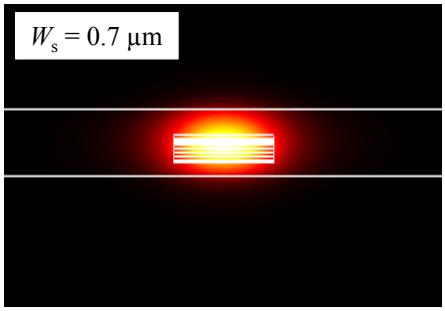

Fig. 2. Mode field profile of a membrane laser with a stripe width of 0.7 μm.

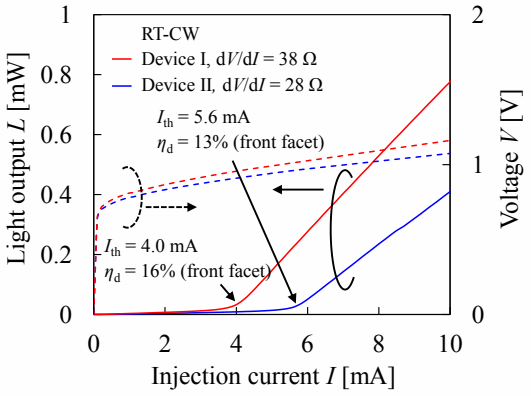

Fig. 3. Current–light output and current–voltage characteristics of membrane FP lasers. In case of the Device. I, a stripe width W_s and cavity length L are 0.6 μm and 830 μm, respectively. In case of Device. II, W_s and L are 0.7 μm and 900 μm.

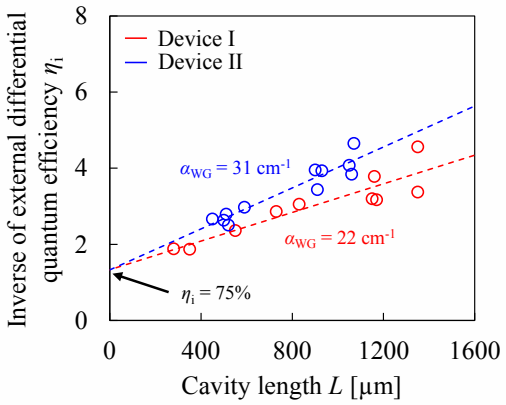

Fig. 4. Measured cavity length dependence of the inverse of the differential quantum efficiency.

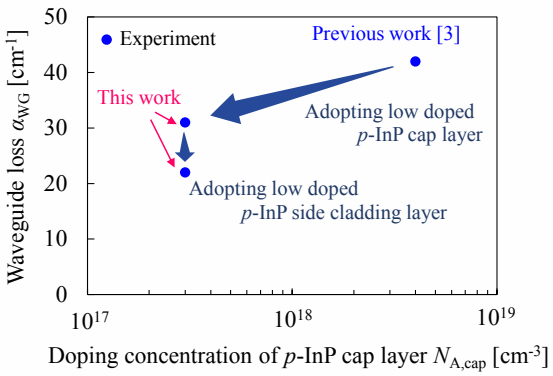

Fig. 5. The waveguide loss dependence on the doping concentration of p-InP cap layer.

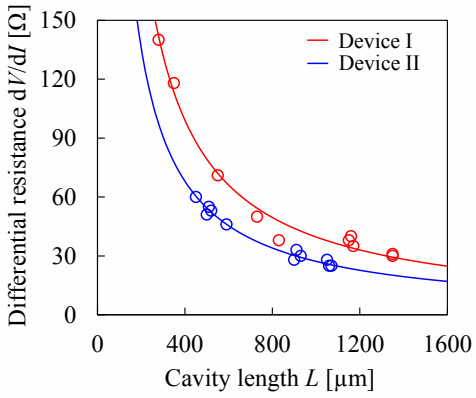

Fig. 6. Measured and fitting curve of cavity length dependence of the differential resistance.